An improved Cellular Automata model to simulate the behavior of high density crowd and validation by experimental data

Claudio Feliciani[a,*], Katsuhiro Nishinari[a,b]

[a] *Research Center for Advanced Science and Technology, The University of Tokyo, 4-6-1 Komaba, Meguro-ku, Tokyo 153-8904, Japan*
[b] *Department of Aeronautics and Astronautics, Graduate School of Engineering, The University of Tokyo, 7-3-1 Hongo, Bunkyo-ku, Tokyo 113-8656, Japan*

Abstract

In this article we present an improved version of the Cellular Automata floor field model making use of a sub-mesh system to increase the maximum density allowed during simulation and reproduce phenomena observed in dense crowds. In order to calibrate the model's parameters and to validate it we used data obtained from an empirical observation of bidirectional pedestrian flow. A good agreement was found between numerical simulation and experimental data and, in particular, the double outflow peak observed during the formation of deadlocks could be reproduced in numerical simulations, thus allowing the analysis of deadlock formation and dissolution. Finally, we used the developed high density model to compute the flow-ratio dependent fundamental diagram of bidirectional flow, demonstrating the instability of balanced flow and predicting the bidirectional flow behavior at very high densities. The model we presented here can be used to prevent dense crowd accidents in the future and to investigate the dynamics of the accidents which already occurred in the past. Additionally, fields such as granular and active matter physics may benefit from the developed framework to study different collective phenomena.

Keywords: bidirectional pedestrian flow, cellular automata, fundamental diagram, simulation, deadlock formation

*Corresponding author:
Email address: feliciani@jamology.rcast.u-tokyo.ac.jp (Claudio Feliciani)

1. Introduction

Dynamic of human crowds exhibits many mysterious and fascinating aspects which have attracted researchers of several disciplines. In particular, the processes leading to the occurrence of accidents in dense crowd are still not completely understood and ways to prevent those situations are mostly summarized as general guidelines and generic constructional norms.
Studies on the dynamic of human crowds stretch many decades back, but it is only in the last decades that researchers have focused on computer simulations to predict the behavior of pedestrians in a vast range of scenarios. Motivation for the use of numerical simulation lies in the fact that it is possible to study scenarios which could not be reproduced experimentally, either because of the risks related to potential injuries or because of the difficulties arising in hiring a large number of participants during supervised experiments (in order to obtain significant experimental data several hundred people are required, but reported studies usually employed few hundred or even less participants [1, 2, 3, 4], while simulations can deal with several thousand people).
Most of the models used for dense crowd are based on physical principles, with granular and active matter physics having the largest contribution [5, 6, 7]. In some case (especially when the crowd is not extremely dense) fluid-dynamic was found being accurate enough to describe macroscopic pedestrian motion. In addition, statistical mechanics and theories based on many-body systems have been useful to understand the characteristics of crowds composed of a large number of people. In this regard, research on pedestrians dynamic has a mutual relationship with research on collective phenomena, with discoveries in both disciplines contributing to the overall understanding.
In particular, because of the difficulties arising in obtaining realistic data during supervised experiments (considering that participants are aware that an experiment is being carried out) and the privacy concerns related with the use of public surveillance cameras for empirical observations, granular matter physics has been useful in gaining precious experimental evidence of different situations; especially in the case of evacuation through a narrow exit [8, 9, 10, 11].
However, granular matter physics is not always directly comparable with

human crowd. Therefore, considering the above reasons, research on extreme scenarios (deadlock, bottlenecks, accidents, panic outbreak,...) has been mostly focused on two directions: computer simulations and research involving animals, which enable to reproduce dangerous scenarios while minimizing the ethical and juridical concerns (in this context experiments have been reported using different sort of animals [12, 13, 14, 15]).
Numerical models used in computer simulations can be divided into continuous and discrete models (although different categorization criteria may be considered). To the former ones belong the fluid-dynamic methods [16, 17, 18] and the social force model [19, 20]. Among discrete models, multi-agent systems [21, 22, 23] and Cellular Automata (CA) [24, 25, 26] are the most widely used.
In some cases simulation models were validated using realistic empirical data gained from supervised experiments under low densities. In particular previous experimental research has dealt with bidirectional counter-flow [2, 4, 27], cross-flow at intersections and evacuation through an exit door [28, 29].
In this study we will focus on the CA model, because of its simplicity and its capability to easily include behaviors observed on pedestrians in real situations. CA has proven being a powerful tool to describe collective pedestrian behavior in many scenarios and its relative simplicity and the limited number of rules implemented in it allows very short computational time. Various phenomena observed in reality could be described using CA models, including the arching at the exit door [30], lane formation [31] and the faster-is-slower effect [32]. However, because of the constraints imposed by the use of a discrete mesh, special models had to be developed to overcome some of the limitations. In this frame a real-coded lattice gas model [33] was derived to improve the accuracy of diagonal motion, a force field was added to assess the potential danger in a dense crowds [34], different velocities were included to account for the velocity distribution usually observed in pedestrians [35, 36] and a finer mesh was proposed to increase the spatial accuracy [25].
However, CA has still the limitation of allowing simulation only for a limited density, namely the one imposed by the size of its mesh, typically set at 0.4 m $\times$ 0.4 m [37]. When each cell of the model has been filled, the maximum density allowed by CA is reached. In general, the mesh used in CA models is sufficient for simulating most of the scenarios observed in pedestrian crowds. In particular, free-flow is accurately modeled and lane formation observed in reality is reproduced in simulation with satisfactory accuracy. On the other hand, in congested situations, local densities may go beyond the limit im-

posed by the CA mesh. Densities up to 8.4 persons m^{-2} have been reported [38] in controlled experiments (under safe conditions), implying that higher densities (possibly higher than 10 persons m^{-2}) can be observed in panicking crowds resulting in injuries or death.
In this study we present a sub-mesh implementation of the CA model which increases the mobility of the pedestrians in dense crowd, thus allowing the simulation of highly congested scenarios. Different sub-mesh approaches have been reported in relation with the Boltzmann lattice used in fluid-dynamic [39, 40, 41], but the method reported here represents a new approach which enables to overcome the low-density limits imposed by the use of the standard discrete mesh in CA.
In order to validate the model we compared the simulation results with experimental data obtained during morning rush hour in a crowded subway station in central Tokyo.
Given the interdisciplinary approach used, applications of the model presented here go beyond the field of pedestrians dynamics and granular matter physics in particular may benefit from it, especially for research related to phenomena like percolation, aggregation and diffusion.

2. Model description

In the case of pedestrian bidirectional flow, the use of a discrete mesh in CA models results in a limited mobility for colliding pedestrians. As a consequence, even at low flows, a complete stop may be observed when pedestrians coming from both directions encounter [42]. To avoid this problem, some authors proposed to introduce an exchange probability to avoid head-on conflicts [24, 43]. This solution works well in a way that pedestrians are less likely to get stuck in front of each others. However, if the exchange probability is set too high, the model tends to overestimate the capability of pedestrians to get through a crowd coming from the opposite direction. On the other hand, when set too low, the full stop previously discussed may easily occur. To overcome this problem, and to correctly reproduce the behavior observed in dense crowds, we decided to introduce some changes to the original CA mesh.
In fact, although most of the fundamental rules governing pedestrian motion are independent on the environment, the very limited visibility found in dense crowds strongly affects pedestrians' mobility, thus requiring a different treatment compared to free-flow conditions.

In particular, we tried to reproduce the pushing behavior usually observed when a deadlock is formed in bidirectional flow. In reality, we observed that people usually stop once they are not able to continue further, but, after a while, they try to find out a route through the opposite coming crowd. By doing so, they move through the dense crowd hoping to get out from the opposite side as soon as possible.
In our model, we gave therefore the pedestrians the possibility to find a way through the crowd by using some additional positions created in the mid of adjacent cells.
The standard mesh used in CA in the case of Neumann neighborhood is given in Figure 1(a) (Manhattan metric was used to compute distances). The center of each cell is given in dark dots and each cell is delimited by border lines. By using the totally asymmetric simple exclusion process (TASEP) only one pedestrian per cell is allowed and thus each cell can be empty or occupied by only one pedestrian at its center.
In our sub-mesh implementation (represented in Figure 1(b)) we introduced additional nodes located in the middle of adjacent cells. Coherently with the use of a Neumann neighborhood we prevented the edges of the cells from being used as sub-mesh locations and we limited the sub-mesh positions to the center of each side.
Even in the sub-mesh implementation TASEP rules apply and therefore a maximum of one pedestrian is allowed in each position. By using the improved model a maximum number of 3 pedestrians per cell is theoretically allowed (one at the center and a total of 2 at the sub-mesh boundaries, considering that pedestrians lying at the boundaries are shared with neighbor cells).

By only creating additional positions we would simply have a CA model with finer mesh and the maximum allowed density would reach 18.75 persons m^{-2} (3 times the normal density of 6.25 persons m^{-2} in the case of a 0.4 m $\times$ 0.4 m mesh). However, we want to set the maximum density allowed in our model to about 10 persons m^{-2}, avoiding unrealistically high densities. This would not be possible in a standard CA model without changing the mesh size.
As introduced above, the motivation for using the sub-mesh structure is not only about increasing the maximum density, but we also want to account for the different behavior found in low and high-density crowds. In fact, once inside a dense crowd, because visibility and mobility quickly degrade, the type of motion usually observed in free flow cannot be recognized anymore.

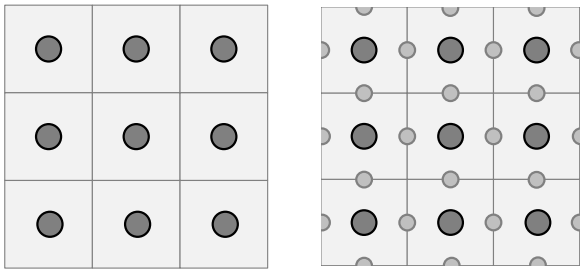

(a) Standard mesh. (b) Sub-mesh implementation.

Figure 1: Neumann neighborhood mesh used in the CA model, standard mesh and the implementation proposed in our study. Overall size of the mesh is unchanged in the sub-mesh approach as sub-locations are introduced in the edges.

After entering a dense crowd cluster, pedestrians simply try to move to the exit in a sort of zigzag motion, without any preference on turning left or right, but only taking any free space they spot nearby.
Therefore, while high density can be simply obtained by scaling the size of the mesh, a more comprehensive approach is required if behavior of the crowd in dense crowd has to be considered. Because we wanted to keep the basic structure of the floor field model (which is successful in predicting low density behavior), we decided to add an overlay grid which can deal with dense crowd. In order to do this a special set of rules which determine under which conditions this additional grid can be used is required.
Keeping in mind that parallel update is used to compute pedestrians' positions, this set of rules is given as follows (a schematic summary is provided in Figure 3) :

1. During free-flow (in case one or more of the neighbor cell are free) pedestrians will move from one center to the other (as schematically illustrated in Figure 2(a)). In the case of the right walking individual (thus moving from left to right) given in Figure 2(a), that pedestrian may move forward, turn right or stay in the same position. In the previous literature some discussion has been made about the necessity to include the back step in bidirectional flow models. Some authors [35, 44, 45] argue that because of the intrinsic nature of bidirectional flow, back stepping has to be avoided and some showed that the use of back stepping will have little influence on the results [43]. On the

other side some authors [46] stressed on the importance of the use of back step to make the model more reasonable. Although experimental observation and personal experience suggest that back stepping should not be required, we decided to introduce it at first. However we found its influence not significant (or negative) and therefore we excluded back stepping in the final model presented here.
Pedestrians select the target cell (forward, left, right or wait/stay) according to the transition which has the highest probability (calculation of this probability will be described later).

2. After having waited a time larger or equal to the maximum waiting time t_{wait} in the same position, if free-flow movement from center to center is still not possible, pedestrians are allowed to move to one of the neighbor sub-mesh locations (see Figure 2(b)). In reality, in this case, a dense crowd has already formed thus limiting the motion of the pedestrians. By giving them the alternative of the sub-mesh, an improved mobility can be achieved.
However, to avoid unrealistic high densities, we limited the use of the sub-mesh by imposing the following additional rule: one pedestrian is allowed to move to a sub-mesh if and only if the total number of pedestrians in the target cell (center plus the four sub-mesh locations) is less than a selected maximum value n_{max}. If n_{max} is set to 1, we will have the standard CA model (only one pedestrian per cell allowed in the center). By setting it equal to 5 each sub-mesh location is used. Values included between 1 and 5 allow to control the maximum local density reached during simulations. Non-integer numbers for n_{max} can be used by creating a floor in which the average n_{max} value corresponds to the sought setting, while each cell takes individual integer values randomly chosen between the upper and lower integer close to n_{max}.
The introduction of the waiting time t_{wait} allows to reduce the walking speed when entering and moving inside a dense crowd (by decreasing the moving frequency, speed is also decreased). In fact, as the waiting time before making the next step must be larger or equal to t_{wait}, by setting $t_{wait} >= 1$ pedestrians have to wait at least one step before moving to each sub-mesh location (the condition pedestrian waiting time $>= t_{wait}$ must be satisfied). Therefore setting $t_{wait} = 1$ means that pedestrians can move every second iteration. As a consequence, although the step length in diagonal motion is longer compared to straight motion, the overall walking speed is reduced because of the

reduced moving frequency.

3. After having moved in a sub-mesh position (corresponding to a dense crowd in reality), pedestrians can move diagonally in a zigzag mode (see Figure 2(c)) by respecting the two rules introduced earlier (i.e. moving only after having waited t_{wait} time steps or more and only if the target cell has a total number of pedestrians lower than n_{max}).
4. If an empty cell-center is spotted, pedestrians can choose to move there directly (without waiting) as in the case of free-flow (see Figure 2(d)). Again, as in all the other cases, the maximum total number of pedestrians per cell n_{max} cannot be exceeded. In case both a sub-mesh and a cell-center pedestrians aim to move to a free cell-center, priority is given to the sub-mesh pedestrian. This is related with the observation that pedestrians leaving a dense crowd tend to be more motivated in moving forward compared to pedestrians which are just trying to enter the crowd.
   As an exceptional case, a back-step is allowed in this case, but only after waiting longer than $t_{wait} + 1$. We found this necessary to avoid the formation of local jam clusters, which require the half back-step to dissolve. However, even in the most congested situation, the use of this option accounted for about 2% of the total distance traveled.
   After re-entering a low-density region by moving to a cell center, pedestrians can move again in a free-flow motion by walking from center to center during each time step.

Calculation of the transition probability is performed based on the floor-field model. Two fundamental fields are used for this calculation: a static floor field, which is based on the distance from the exit or the destination, and a dynamic floor field, which is based on a virtual trace (a sort of pheromone) left by pedestrians during movement (a detailed description of the floor-field model in case of pedestrian bidirectional flow is given in [4]). This virtual trace left by moving pedestrians can decay with time and diffuse to neighbor cells (for a detailed description of the dynamic floor field [47] is suggested). In addition to the classical static and dynamic floor fields, to increase the accuracy of our model, we used the anticipation [4] and the wall [47] floor fields. Therefore, by considering the different floor-fields and the TASAP exclusion rule, the transition probability for a cell (center) at position i, j can be computed as:

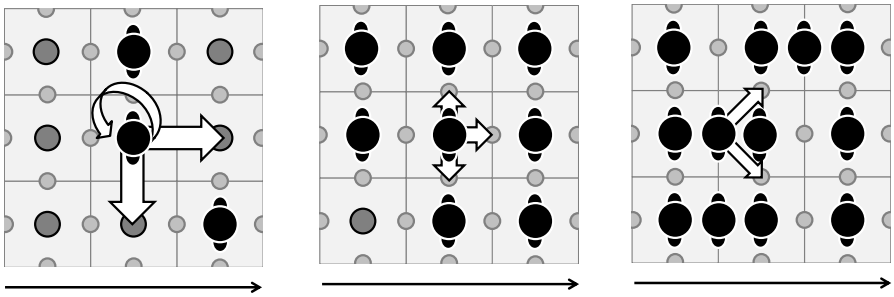

(a) Motion in case of free-flow.

(b) Start pushing after having waited long enough.

(c) Moving inside a dense crowd.

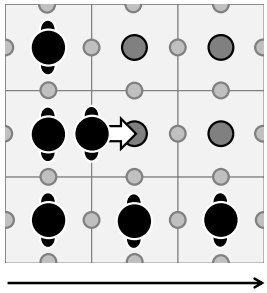

(d) Leaving the dense crowd.

Figure 2: Pedestrian's motion in case of a dense crowd by using the sub-mesh implementation.

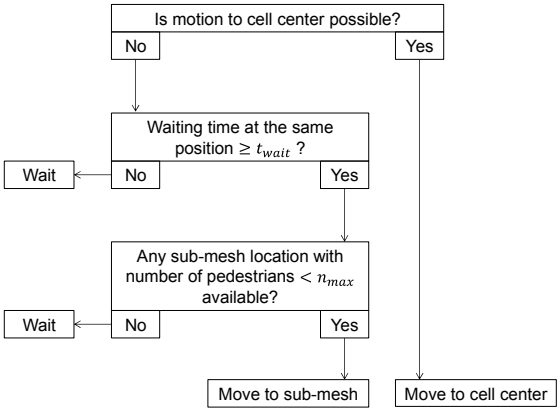

Figure 3: Schematic review of the transition rules in the sub-mesh implementation.

$$\begin{aligned} p_{i,j} =& N\xi_{i,j} \exp(-k_S S_{i,j}) \exp(k_D D_{i,j}) \exp(-k_A A_{i,j}) \\ & \exp(k_W W_{i,j})(1 - \phi_{i,j}) \end{aligned} \tag{1}$$

with N being the normalization parameter, $\xi_{i,j}$ the obstacle parameter (0 if cell (i, j) is a wall or obstacle cell, 1 otherwise), $S_{i,j}$, $D_{i,j}$, $A_{i,j}$, $W_{i,j}$ the values of the static, dynamic, anticipation and wall floor fields, k_S, k_D, k_A, k_W their corresponding sensitivity parameters and $\phi_{i,j}$ the occupancy parameter. In the case of the sub-mesh implementation the occupancy parameter will be 0 if the number of pedestrians in all the positions of cell (i, j) is less then n_{max} and 1 otherwise. In mathematical notation:

$$\phi_{i,j} = \begin{cases} 0, & \text{total pedestrians in cell } (i,j) < n_{max}. \\ 1, & \text{otherwise.} \end{cases} \tag{2}$$

In the case of sub-mesh, the transition probability is a combination of the floor-field values of the adjacent cells.

Considering Figure 4 with a right-walker in the center, the transition probability for a left turn can be computed as:

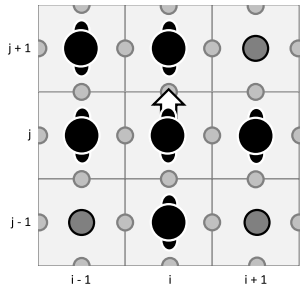

Figure 4: Transition probability in the case of sub-mesh motion.

$$
\begin{aligned}
p_{i,j+\frac{1}{2}} =& N\xi_{i,j+\frac{1}{2}} \exp(-k_S \frac{S_{i,j} + S_{i,j+1}}{2}) \\
& \exp(k_D \frac{D_{i,j} + D_{i,j+1}}{2}) \exp(k_W \frac{W_{i,j} + W_{i,j+1}}{2}) \\
& (1 - \phi_{i,j+1})
\end{aligned}
\tag{3}
$$

with the notation being the same of the previous equation and index $\frac{1}{2}$ indicating the position of the sub-mesh location. This means that the transition probability for a left turn to the left sub-mesh will be given by the transition probability computed by using the average value of the different floor-fields in the current and the left target cell. The same apply to the right and the forward sub-cells. In other words, the pedestrian will move to the sub-mesh closest to the cell that would have the highest transition probability if empty.
It has to be remarked that the anticipation floor field was omitted in the above equation; the obvious reason being that the anticipation of movements for the pedestrians coming in the opposite direction makes no sense in a dense crowd with very limited visibility.
Finally, we decided to keep the exchange probability used in some CA models. However, to adapt it to our model, we used the following special rules:

1. A pair of pedestrians heading to opposite destinations (here left and right walkers) may choose to exchange their position (see Figure 5) with a probability $p_E \in \{0, 1\}$ only after having waited at the same position a total time greater than $2 \cdot t_{wait}$ time steps. For this reason, the exchange probability used here is different from the one previously used in other

studies. Here, even setting an exchange probability equal to 1 will not result in an instantaneous exchange, because a pair of pedestrians will have to wait more than $2 \cdot t_{wait}$ time steps before being allowed to consider an exchange (the value of 2 has been chosen intuitively based on the fact that 2 pedestrians are involved). By setting t_{wait} relatively large, pedestrians are likely to move to alternative locations before considering a position exchange.

2. Position exchange can take place for a pair of opposite walking pedestrians which are both at the center or alternatively in the center and in one sub-mesh position. In case 3 pedestrians are aligned in both cells' center and the middle sub-mesh, then exchange takes place only for the pairs located at minimum distance (cell center/sub-mesh pair).

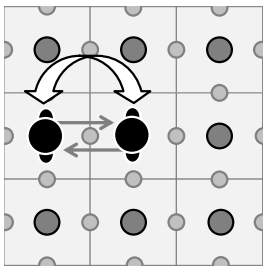

Figure 5: Cell exchange for pedestrians having opposite destination.

The use of the position exchange rule may seem in contrast with the sub-mesh system presented here. In fact, setting n_{max} sufficiently high, complete stops are very unlikely to occur. However, we observed that adding the exchange probability to our sub-mesh model can increase the accuracy of the results, both from a qualitative and quantitative point of view (details will be discussed in the results section).
This can be explained considering the fact that the sub-mesh implementation allow a temporary increase in local density and enhance the mobility in dense crowd, but it is a relatively slow process acting as a buffer accumulating pedestrians coming from opposite directions. A combination with the position exchange allows keeping the maximum density to reasonable limits while providing a solution to quickly dissolve the crowd.
Update procedure is performed using the parallel-update rule [48], i.e. target position is reserved before actually moving each pedestrian. In case of con-

flict, i.e. multiple pedestrians wishing to move to the same position, one of the pedestrians targeting that position will be chosen with equal probability. The scheme followed in the simulation process is summarized in Figure 6.

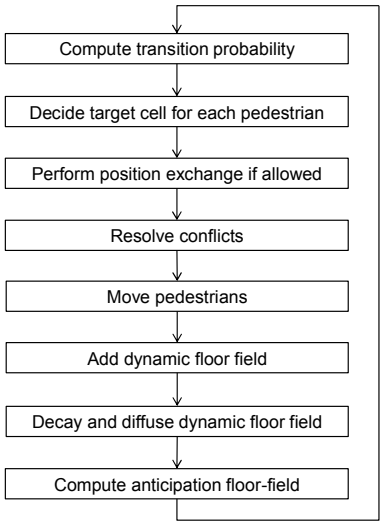

Figure 6: Process flowchart for the simulation of pedestrian's bidirectional flow.

At first, for each pedestrian, its corresponding transition probabilities are computed. Based on these probabilities a target cell is chosen (this may be its current cell if the current position results having the highest probability). Later, pedestrians which are eligible for position exchange are identified and exchanges eventually take place. As a next step, conflicts for the same position are resolved and pedestrians are moved into their new position. In the final steps the dynamic floor field is added and later decayed and diffused. Finally, the anticipation floor field which will be used in the next time step is computed.

3. Parameters estimation and simulation results

A bidirectional flow model using the rules described above was implemented in the NetLogo open source software [49]. The model consisted of an horizontal corridor 6.2 m in width and 12.2 m in length. Pedestrians can enter on one side of the corridor and leave from the other side, thus forming

either unidirectional (when pedestrians enter only from one side) or bidirectional flow. Because two kind of walkers are present in the model, namely left- and right-walkers, two different static fields had to be used. The static field of left walkers decreases from right to left and reaches a value of 0 at the exit on the left side. The static field for right walkers acts in the opposite direction, decreasing from left to right and becoming 0 in the exit at the right side. Dynamic field is also specific to each type of walker, reproducing the fact that pedestrians going in one direction follow only other pedestrians walking in the same direction. On the other side, the anticipation field acts between the two different kind of pedestrians, with left-walkers trying to avoid collisions with right-walkers and the opposite situation. Finally, the wall field is the same for both type of walkers, as both left- and right-walkers try to avoid being too close to the wall.

In order to estimate the parameters to be used in the model, data obtained from an empirical observation were employed for calibration. A corridor-like section in a subway station in central Tokyo was analyzed during rush-hour to obtain the bidirectional flow resulting in the narrow section considered (details for the empirical data acquisition and treatment are given in [50] [1]). A small difference exists between the geometry of the corridor used during empirical observation and the model used for simulation, with the corridor referring to experimental data being slightly larger on the left side. However, since congestion was observed in the right side of the corridor (where the width is the same in both experimental and numerical models), the approximation used in the numerical model (with both sides having equal width) can be considered accurate enough to correctly reproduce the phenomena observed in reality.

The empirical data set consists of in- and outflow data for the observed corridor at different moments during the rush-hour period considered. To estimate the parameters to be used in the numerical simulation model, we used the experimental inflow on each side of the corridor as simulation input and we computed the outflow resulting in the exit located at the opposite side. Results for the total in- and outflow and the density under normal and crowded conditions are given in Figure 7 and Figure 8 respectively.

[1] Note: not all the results presented in the empirical study could be used for comparison with simulation, because, in some cases, lanes partially formed before the entrance of the corridor, thus making the setup of boundary conditions unfeasible.

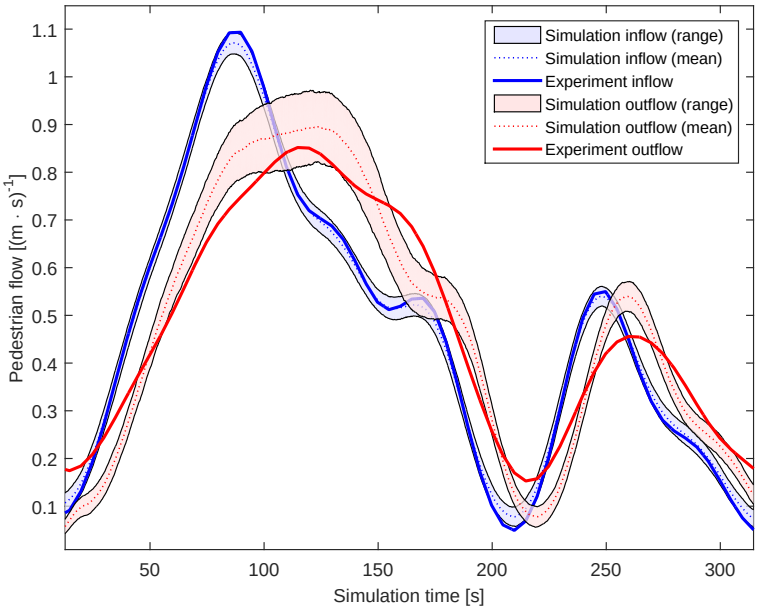

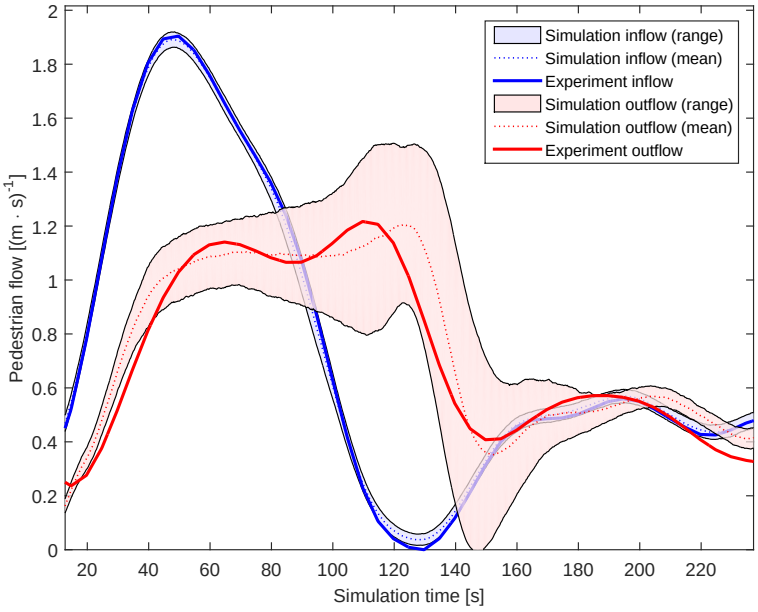

(b) Dense crowd (deadlock formation or full stop)

Figure 7: Comparison between experimental and simulated flow.

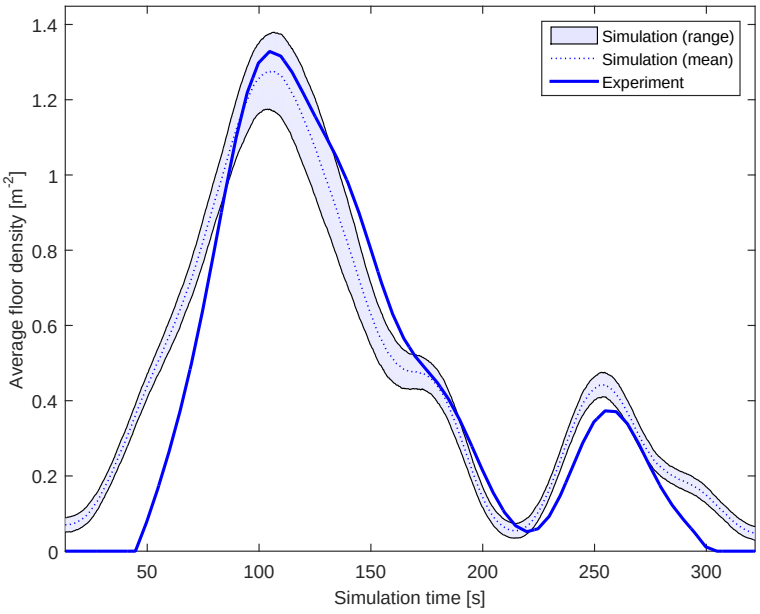

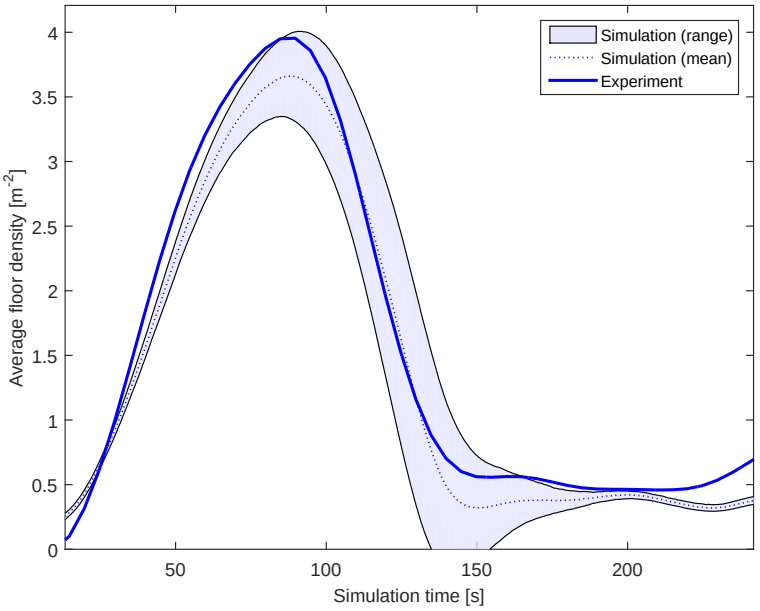

(b) Dense crowd (deadlock formation or full stop)

Figure 8: Comparison between experimental and simulated floor density.

The dotted blue line represents the average simulation result, with the blue region along it giving the standard deviation resulting from the several simulation runs (500 for each case). The bold blue line is the experimental result recorded during observation. Simulated density here is defined as the overall number of pedestrians in the corridor section divided by the total surface of the corridor itself; in- and outflow is intended as the sum of each quantity on both sides of the corridor. Experimental density is derived from the cumulative curves representing the cumulative total number of pedestrians which entered and left the section analyzed, considering that the corridor was empty at the beginning (for details see [50]).
In the case of flow results, it is important to remark that although the experimental inflow is taken as input for the simulation, some small differences exist between the inflow actually achieved during simulation and the one expected. This can be explained considering the fact that experimental flow curve was filtered to remove sampling noise, thus resulting in a continuous graph. In the numerical model, to reproduce a given flow, a discrete number of pedestrians need to be introduced, which may result in small differences between expected and obtained curves. This is particularly visible for sudden inflow changes at low inflow levels, such between consecutive peaks. In general, however, differences between the cumulative must-be inflow and the one obtained accounted for less than 1-2%.
Dotted red lines in Figure 7 represent the average outflow obtained from simulation with the background being the standard deviation resulting among all simulations runs. The thick red line represents the experimental result.
As shown in Figure 7 and Figure 8, in general, a relatively good agreement is found between experimental and simulation results, with agreement of the density curves being particularly good. Qualitatively the most relevant changes are correctly reproduced in all the cases, with the quantitative values being also in satisfactory agreement. In particular, the double peak observed during the formation of deadlock is reproduced in the numerical simulation (see Figure 7(b)), although the changes between both peaks appear smaller compared to the experimental result (especially concerning the decrease of the outflow, which, although observed in simulation, is much smaller compared to the experimental result).
This characteristic could be reproduced due to the higher mobility given by the sub-mesh model presented here. In fact, although overall density reaches about 4 persons m^{-2}, during the formation of deadlock (see Figure 8(b)), local densities were higher than 6 persons m^{-2}. In this regard, the sub-mesh

implementation was found being a useful method to allow motion under dense crowd conditions, although its efficiency for higher densities (above 6 persons m^{-2}) or different geometrical configurations has to be checked if new experimental data for those conditions will become available.
It is important to remark that a slightly different set of parameters had to be used for the two cases, for which values are given in Table 1. Free walking velocity was set at 1.4 m/s to correspond with the measurement performed during the observation and in line with the values reported in the literature under similar conditions [51, 37].

Table 1: Parameters used in the simulation model for the different scenarios. The 2.8-value for n_{max} was obtained by setting different n_{max} values for each cell (namely 2 or 3) and having the floor average corresponding to the sought setting.

Parameter	Normal conditions	Dense crowd
k_S	8.5	13.0
k_D	6.0	
α_D	0.25	
β_D	0.25	
k_A	8.5	13.0
d_A	4	
k_W	0.75	
p_E	0.23	0.35
n_{max}	2.8	
t_{wait}	1	

In Table 1 k_S, k_D, k_A, k_W, p_E, n_{max} and t_{wait} are the model's parameters described in the previous section, while α_D and β_D are respectively the diffusion and decay of the dynamic field and d_A is the anticipation distance (for details refer to [4]).
The parameters which had to be adapted depending on the situation are all related to the way pedestrians behave under different conditions. In particular it can be observed that a large k_S had to be used in dense crowd (when a deadlock was formed). This can be explained by considering the fact that in order to cross the corridor, pedestrians need to counteract the pressure formed by the large counter-flow. In other words more effort is required to cross the corridor under congested dense crowd compared to normal conditions. It can be observed however, that the required increase of k_S is related

with the maximum observed inflow (being slightly less than double). In this sense, linking the parameter k_S with the incoming flow may be useful in obtaining a model capable of accurately simulate different scenarios.
Parameter k_A, related with the anticipation floor field, had to be adapted to the different flow conditions as well. Interestingly we found that, by setting k_A equal to k_S, besides obtaining quantitative good results a fairly natural behavior can be observed during simulation by following the motion of pedestrians. In this regard, the sensitivity parameters which need to be adjusted can be reduced to one as k_A can be safely set equal to k_S.
Finally, exchange probability p_E had to be adapted to the different conditions to account for the fact that close position exchange occurs more frequently in dense crowd compared to low density conditions. Again, the optimal parameters found for p_E in both cases show a relationship similar to the ratio of the maximum inflow observed in the main peak. This may suggest that the most important parameters have a relationship with the total incoming flow. However, a more detailed investigation would be required to confirm this fact.
We can now look more in detail into the behavior of pedestrians in different situations. First we wish to analyze the motion of pedestrians under normal conditions, like in the scenario considered in Figure 7(a). Considering that the simulation is performed stepwise, the movement at each iteration can be categorized as follows:

1. Forward motion: direction did not change from the previous iteration.
2. Waiting: position has not changed since the previous iteration.
3. Rotating: position and direction are different compared to the last moving iteration.
4. Position exchange: pedestrian changed its position with someone else.

When a pedestrian leaves the corridor the number of steps for each action are converted into time and those figures are combined with other pedestrians leaving at the same time. In Figure 9 is represented the average time required to cross the corridor from side to side divided into the different actions given above.

The total crossing time is the average time required to cross the corridor from side to side and can be obtained by summing up the time necessary for the different actions. It clearly grows up when a large counter-flow is encountered. The time spent moving forward is almost constant because most of the pedestrians move forward for a distance which is close to the horizontal

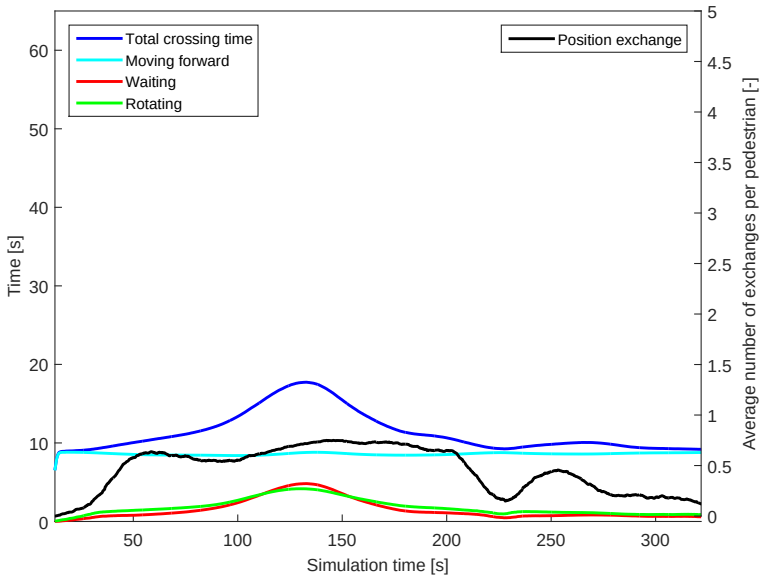

Figure 9: Average time required for different actions while crossing the corridor in normal conditions.

distance of the corridor (free walking speed is constant in our model). Small variations can be observed in case one pedestrian will have to walk for a short distance toward the wall to a avoid a collision, thus walking forward for a longer distance compared to the minimum required to cross the corridor.
Concerning the waiting and rotation times, it can be observed that they both follow a common path by peaking in the most crowded moment. The increase in overall crossing time can therefore be attributed to an increase of both values.
Finally, we wish to consider the average number of position exchanges required to cross the corridor for each pedestrian, given by the the black line in Figure 9 (with the corresponding scale given on the right side). Clearly, during normal conditions, position exchange is not a relevant phenomenon (less than one position exchange is observed on average).
We can now analyze the more crowded scenario (Figure 7(b)), for which the behavioral timing analysis is given in Figure 10. As one would expect, during the formation of deadlock the overall crossing time grows, eventually requiring about one minute to cover the corridor distance in the worst situation.

It is interesting to notice that there is a substantial difference between the scenario illustrated in Figure 9 and Figure 10. In fact, during deadlock

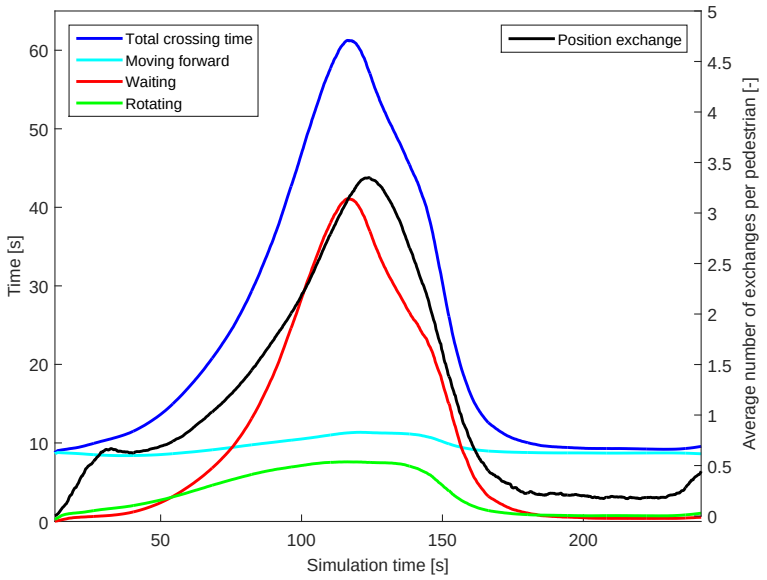

Figure 10: Deadlock formation analyzed using the time required for different actions.

formation waiting time and rotation time are not coupled anymore. As indicated in Figure 10 at first there is a steep increase of the waiting time, which later eventually decreases in a two 2-steps fashion. On the other side the rotation time slowly grows from the beginning of the deadlock formation throughout the whole duration, until finally quickly dropping when the deadlock is dissolved. This indicates that the dissolution of a deadlock is related to an increased mobility of the pedestrians, while its formation is connected with a large number of people having to stop to avoid collisions. Consequently, guiding pedestrians along preferential directions may be useful in avoiding the initial stop created by the incoming large counter-flow.
During deadlock formation position exchange plays a more important role (compared to the previous case), with a maximum value of about 3 position exchanges reached during the maximum flow. This shows that although the increased mobility given by our model, exchange probability cannot be completely ruled out.

4. Extended bidirectional flow fundamental diagram

We will now use the simulation model developed here to obtain some complex fundamental diagrams for bidirectional flow.

First, we wish to compare the fundamental diagram obtained by simulation with experimental results from the literature. By using the model described above we performed simulations for a balanced bidirectional flow by changing the inflow setting from 0.05 to 2.50 persons / m $\cdot$ s (in 0.05 $(\mathrm{m{\cdot}s})^{-1}$ steps). Parameters for the dense crowd were used here and simulations were each performed for a total time corresponding to 5 minutes in the reality (with computational time being clearly much shorter). Resulting total outflow and density were recorded in the fundamental diagram and simulation results were compared with the semi-experimental data provided by Weidmann [37] in his meta-study (see Figure 11) [2].
The fundamental diagram of Weidmann has been chosen among the several ones available in the literature because of the following reasons:

1. It is the only one that provides data for relatively high densities, i.e. above 4-5 persons m^{-2}, while most of the experimental studies are limited to free flow scenarios with densities below 2-3 persons m^{-2}.
2. It has been widely used in the literature as reference and, although its accuracy has been debated [36, 52], its widespread use allows a prompt comparison with results from different studies.

A good agreement between both data sets is found for densities below about 5 persons m^{-2}, with the results from simulation being slightly higher than the data by Weidmann. For higher densities the flow given by Weidmann quickly drops to 0, while the simulation's results only slightly decreases keeping a small flow even under high density conditions. We will discuss about this aspect below, but it is important to remember that the result given by Weidmann is based on a collection of experimental data and it is assumed (without being strictly verified) that for densities above around 5 persons m^{-2} motion is not possible.
Finally, we computed the fundamental diagram by changing the flow ratio of bidirectional flow from 0 to 1 in steps of 0.1 (total inflow values were the same as above, from 0.05 to 2.50 persons / m $\cdot$ s). Flow ratio is the amount of flow in one direction divided by the total flow from both directions. If we define:

[2]Note: data used for comparison refer to the semi-empirical results reported by Weidmann and not the equation which fits those data. Flow is obtained by multiplying density with velocity.

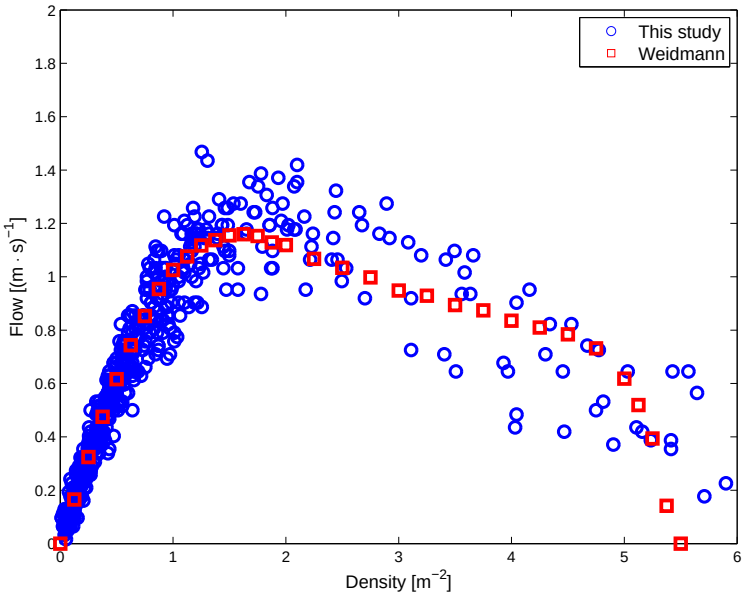

Figure 11: Comparison of the numerically simulated bidirectional flow fundamental diagram with the data by Weidmann.

$$r_{L\to R} = \frac{J_{L\to R}}{J_{L\to R} + J_{R\to L}} \tag{4}$$

$$r_{R\to L} = \frac{J_{R\to L}}{J_{L\to R} + J_{R\to L}} \tag{5}$$

being the flow ratio from left to right and right to left respectively (J is the flow in the given direction), it can be easily obtained that:

$$r_{L\to R} + r_{R\to L} = 1 \tag{6}$$

Flow ratio is therefore symmetric around 0.5 (perfectly balanced flow) and for this reason we decided to summarize all results in a 0 to 0.5 scale (and to make visualization clearer). Results for the flow-ratio dependent bidirectional flow fundamental diagram are given in Figure 12.

The fundamental diagram presented here shows a qualitatively good agreement with the one reported by Alhajyaseen et al. [53, 54] for the case of crosswalks, which, although different in constitution, have common properties with corridors. Clearly, balanced bidirectional flow is the one performing

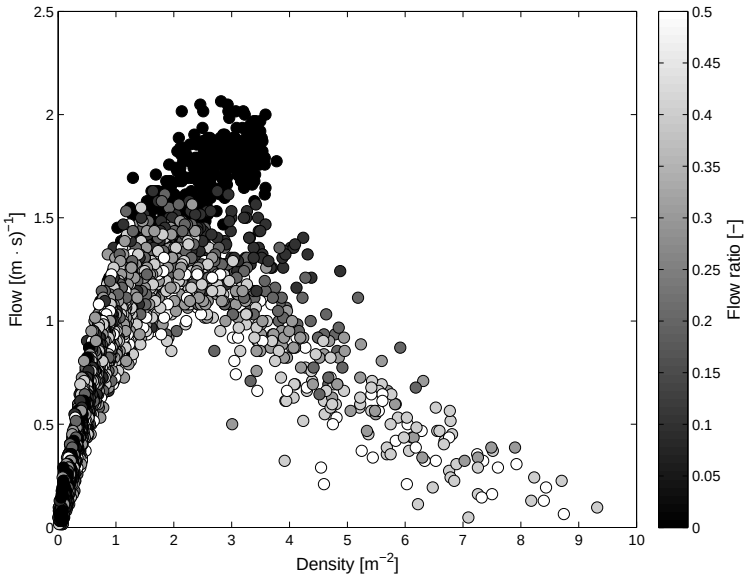

Figure 12: Bidirectional flow fundamental diagram and its relationship with flow ratio.

the worst as reported by different authors [2]. Unidirectional flow show a stronger stability, without decaying into congested motion for the 5 minutes duration of the simulations. In general, as the flow ratio approaches 0.5, instability grows, with congestion occurring earlier.

As Figure 12 shows, a very small outflow is recorded even in extremely dense crowd (above 6 persons m^{-2}). This is a consequence of the fact that p_E is small, but still larger than 0 in our model, thus allowing few pedestrians to cross the corridor even during very crowded scenarios. During the simulation a percolation-like behavior was observed for such densities, with a only limited number of people being able to cross the corridor after a long time. The fact that results can be produced even for such high densities clearly show the theoretical capability of our model to deal with very dense crowd. However, although some authors reported that pressure waves form at very high density [55], thus leading to some sort of very limited flow, there is no experimental quantitative evidence to verify the results under such extreme conditions. In this regard we hope that empirical data will become accessible in the future, thus allowing a critical comparison with the results presented here.

Finally, it has to be remarked that over the long run, if densities keep being

above around 6 persons m^{-2}, more complex psychological phenomena are expected such as frustration, panic or desperation, making an accurate prediction an even more challenging task. In addition, pedestrian may fall down and pile on top of each other, thus creating an extremely dangerous scenario going beyond the modeling capabilities.
Nonetheless, the model presented here gives the possibility to investigate if such high densities may actually occur (even for a short time) and to investigate with higher accuracy accidents which already occurred in the past. From this point of view the high density allowed by the sub-mesh model gives a deeper insight into the formation of dangerous crowd phenomena, thus possibly allowing preventing them in the future.

5. Conclusions

Cellular Automata has been widely used in the frame of pedestrian dynamics simulation. In particular the floor field model has been able to accurately predict different phenomena with good accuracy. However, one of the limitations of the Cellular Automata has been its discrete mesh and the relatively low maximum density associated with it. In this study we presented a modified version of the floor field model making use of a sub-mesh system to allow simulations of very dense crowd and account for the behavior found in such situations. A sub-mesh position located between adjacent cells is added and may be used by pedestrians in dense crowd under particular conditions. As a consequence, maximum densities reached can be higher than the ones obtained in conventional Cellular Automata models. At the same time, dense crowd phenomena can be simulated more accurately.
Comparison between simulation results and experimental data from empirical observations showed a satisfactory agreement both under a qualitative and a quantitative aspect. In particular the characteristic double peak observed during deadlock formation could be reproduced using a numerical model, allowing a further investigation into the reasons leading to this phenomenon. In this regard, we observed that deadlocks form because pedestrians tend to stop in front of a large counter-flow. On the other hand, an increased mobility inside the dense crowd is associated with the dissolution of deadlocks.
The high-density framework has been used to generate an extended fundamental diagram for bidirectional flow, showing that dense crowd simulations are actually possible and confirming the instability of the balanced flow compared to unidirectional motion. However, experimental data for high-density

crowd are required to validate the model under such conditions and/or perform a re-calibration of the parameters used.
Direct applications of this model can be accident prevention and/or investigation of accidents which already occurred in the past. Additionally, the framework presented here may be adapted for an use in different disciplines, with granular and active matter physics being potential candidates.
In the future, new implementations may be required to further increase the accuracy obtained in simulations, for example by considering the distribution of the walking speed or by improving the diagonal motion (for example by adding the use of the corner points to the current model). If experimental data will become available, different scenarios (cross-walk at intersections, evacuation through a small exit,...) could be simulated to validate the model under a large range of situations.

Acknowledgments

This work was financially supported by JSPS KAKENHI Grant Number 25287026 and the Doctoral Student Special Incentives Program (SEUT RA) of the University of Tokyo.

References

[1] T. Kretz, A. Grünebohm, M. Kaufman, F. Mazur, M. Schreckenberg, Experimental study of pedestrian counterflow in a corridor, Journal of Statistical Mechanics: Theory and Experiment 2006 (10) (2006) P10001. doi:10.1088/1742-5468/2006/10/P10001.
URL http://dx.doi.org/10.1088/1742-5468/2006/10/P10001

[2] J. Zhang, W. Klingsch, A. Schadschneider, A. Seyfried, Ordering in bidirectional pedestrian flows and its influence on the fundamental diagram, Journal of Statistical Mechanics: Theory and Experiment 2012 (02) (2012) P02002. doi:10.1088/1742-5468/2012/02/P02002.
URL http://dx.doi.org/10.1088/1742-5468/2012/02/P02002

[3] D. Helbing, L. Buzna, A. Johansson, T. Werner, Self-organized pedestrian crowd dynamics: Experiments, simulations, and design solutions, Transportation science 39 (1) (2005) 1–24. doi:10.1287/trsc.1040.0108.
URL http://dx.doi.org/10.1287/trsc.1040.0108

[4] Y. Suma, D. Yanagisawa, K. Nishinari, Anticipation effect in pedestrian dynamics: Modeling and experiments, Physica A: Statistical Mechanics and its Applications 391 (1) (2012) 248–263. doi:10.1016/j.physa.2011.07.022.
URL http://dx.doi.org/10.1016/j.physa.2011.07.022

[5] Y. Sakuma, M. Imai, Model system of self-reproducing vesicles, Physical Review Letters 107 (19) (2011) 198101. doi:10.1103/PhysRevLett.107.198101.
URL http://dx.doi.org/10.1103/PhysRevLett.107.198101

[6] S. Rafaï, L. Jibuti, P. Peyla, Effective viscosity of microswimmer suspensions, Physical Review Letters 104 (9) (2010) 098102. doi:10.1103/PhysRevLett.104.098102.
URL http://dx.doi.org/10.1103/PhysRevLett.104.098102

[7] T. Vicsek, A. Czirók, E. Ben-Jacob, I. Cohen, O. Shochet, Novel type of phase transition in a system of self-driven particles, Physical Review Letters 75 (6) (1995) 1226. doi:10.1103/PhysRevLett.75.1226.
URL http://dx.doi.org/10.1103/PhysRevLett.75.1226

[8] I. Zuriguel, A. Garcimartín, D. Maza, L. A. Pugnaloni, J. Pastor, Jamming during the discharge of granular matter from a silo, Physical Review E 71 (5) (2005) 051303. doi:10.1103/PhysRevE.71.051303.
URL http://dx.doi.org/10.1103/PhysRevE.71.051303

[9] K. To, P.-Y. Lai, H. Pak, Jamming of granular flow in a two-dimensional hopper, Physical Review Letters 86 (1) (2001) 71. doi:10.1103/PhysRevLett.86.71.
URL http://dx.doi.org/10.1103/PhysRevLett.86.71

[10] J. Tang, R. Behringer, How granular materials jam in a hopper, Chaos-Woodbury 21 (4) (2011) 041107. doi:10.1063/1.3669495.
URL http://dx.doi.org/10.1063/1.3669495

[11] T. Masuda, K. Nishinari, A. Schadschneider, Critical bottleneck size for jamless particle flows in two dimensions, Physical Review Letters 112 (13) (2014) 138701. doi:10.1103/PhysRevLett.112.138701.
URL http://dx.doi.org/10.1103/PhysRevLett.112.138701

[12] S. Boari, R. Josens, D. R. Parisi, Efficient egress of escaping ants stressed with temperature, PLoS ONE 8 (11) (2013) 1–7. doi:10.1371/journal.pone.0081082.
URL http://dx.doi.org/10.1371/journal.pone.0081082

[13] A. Garcimartín, J. Pastor, L. M. Ferrer, J. Ramos, C. Martín-Gómez, I. Zuriguel, Flow and clogging of a sheep herd passing through a bottleneck, Physical Review E 91 (2) (2015) 022808. doi:10.1103/PhysRevE.91.022808.
URL http://dx.doi.org/10.1103/PhysRevE.91.022808

[14] C. Saloma, G. J. Perez, G. Tapang, M. Lim, C. Palmes-Saloma, Self-organized queuing and scale-free behavior in real escape panic, Proceedings of the National Academy of Sciences 100 (21) (2003) 11947–11952. doi:10.1073/pnas.2031912100.
URL http://dx.doi.org/10.1073/pnas.2031912100

[15] E. Altshuler, O. Ramos, Y. Nu, Symmetry breaking in escaping ants, The American Naturalist 166 (6) (2014) 643–649. doi:10.1086/498139.
URL http://dx.doi.org/10.1086/498139

[16] B. Piccoli, A. Tosin, Pedestrian flows in bounded domains with obstacles, Continuum Mechanics and Thermodynamics 21 (2) (2009) 85–107. doi:10.1007/s00161-009-0100-x.
URL http://dx.doi.org/10.1007/s00161-009-0100-x

[17] D. Helbing, A fluid dynamic model for the movement of pedestrians, arXiv:cond-matarXiv:9805213.
URL http://arxiv.org/abs/cond-mat/9805213

[18] R. M. Colombo, M. D. Rosini, Pedestrian flows and non-classical shocks, Mathematical Methods in the Applied Sciences 28 (13) (2005) 1553–1567. doi:10.1002/mma.624.
URL http://dx.doi.org/10.1002/mma.624

[19] D. Helbing, P. Molnár, Social force model for pedestrian dynamics, Physical Review E 51 (1995) 4282–4286. doi:10.1103/PhysRevE.51.4282.
URL http://dx.doi.org/10.1103/PhysRevE.51.4282

[20] A. Seyfried, B. Steffen, T. Lippert, Basics of modelling the pedestrian flow, Physica A: Statistical Mechanics and its Applications 368 (1)

(2006) 232–238. doi:10.1016/j.physa.2005.11.052.
URL http://dx.doi.org/10.1016/j.physa.2005.11.052

[21] S. Bandini, M. L. Federici, S. Manzoni, G. Vizzari, Towards a methodology for situated cellular agent based crowd simulations, in: Lecture Notes in Computer Science (including subseries Lecture Notes in Artificial Intelligence and Lecture Notes in Bioinformatics), Springer, 2006, pp. 203–220. doi:10.1007/11759683_13.
URL http://dx.doi.org/10.1007/11759683_13

[22] X. Pan, C. S. Han, K. Dauber, K. H. Law, A multi-agent based framework for the simulation of human and social behaviors during emergency evacuations, Ai & Society 22 (2) (2007) 113–132. doi:10.1007/s00146-007-0126-1.
URL http://dx.doi.org/10.1007/s00146-007-0126-1

[23] M. C. Toyama, A. L. Bazzan, R. Da Silva, An agent-based simulation of pedestrian dynamics: from lane formation to auditorium evacuation, in: Proceedings of the fifth international joint conference on Autonomous agents and multiagent systems, 2006, pp. 108–110. doi:10.1145/1160633.1160647.
URL http://dx.doi.org/10.1145/1160633.1160647

[24] V. J. Blue, J. L. Adler, Cellular automata microsimulation for modeling bi-directional pedestrian walkways, Transportation Research Part B: Methodological 35 (3) (2001) 293–312. doi:10.1016/S0191-2615(99)00052-1.
URL http://dx.doi.org/10.1016/S0191-2615(99)00052-1

[25] C. Burstedde, K. Klauck, A. Schadschneider, J. Zittartz, Simulation of pedestrian dynamics using a two-dimensional cellular automaton, Physica A: Statistical Mechanics and its Applications 295 (3) (2001) 507–525. doi:10.1016/S0378-4371(01)00141-8.
URL http://dx.doi.org/10.1016/S0378-4371(01)00141-8

[26] A. Kirchner, A. Schadschneider, Simulation of evacuation processes using a bionics-inspired cellular automaton model for pedestrian dynamics, Physica A: Statistical Mechanics and its Applications 312 (1) (2002) 260–276. doi:10.1016/S0378-4371(02)00857-9.
URL http://dx.doi.org/10.1016/S0378-4371(02)00857-9

[27] M. Isobe, T. Adachi, T. Nagatani, Experiment and simulation of pedestrian counter flow, Physica A: Statistical Mechanics and its Applications 336 (3–4) (2004) 638–650. doi:10.1016/j.physa.2004.01.043.
URL http://dx.doi.org/10.1016/j.physa.2004.01.043

[28] A. Kirchner, H. Klüpfel, K. Nishinari, A. Schadschneider, M. Schreckenberg, Simulation of competitive egress behavior: comparison with aircraft evacuation data, Physica A: Statistical Mechanics and its Applications 324 (3) (2003) 689–697. doi:10.1016/S0378-4371(03)00076-1.
URL http://dx.doi.org/10.1016/S0378-4371(03)00076-1

[29] D. Yanagisawa, R. Nishi, A. Tomoeda, K. Ohtsuka, A. Kimura, Y. Suma, K. Nishinari, Study on efficiency of evacuation with an obstacle on hexagonal cell space, SICE Journal of Control, Measurement, and System Integration 3 (6) (2010) 395–401. doi:10.9746/jcmsi.3.395.
URL http://dx.doi.org/10.9746/jcmsi.3.395

[30] Z. Daoliang, Y. Lizhong, L. Jian, Exit dynamics of occupant evacuation in an emergency, Physica A: Statistical Mechanics and its Applications 363 (2) (2006) 501–511. doi:10.1016/j.physa.2005.08.012.
URL http://dx.doi.org/10.1016/j.physa.2005.08.012

[31] M. Kaufman, Lane Formation in Counterflow Situations of Pedestrian Traffic, Master's thesis, Duisburg-Essen University (2007).

[32] S. Wei-Guo, Y. Yan-Fei, W. Bing-Hong, F. Wei-Cheng, Evacuation behaviors at exit in ca model with force essentials: A comparison with social force model, Physica A: Statistical Mechanics and its Applications 371 (2) (2006) 658–666. doi:10.1016/j.physa.2006.03.027.
URL http://dx.doi.org/10.1016/j.physa.2006.03.027

[33] K. Yamamoto, S. Kokubo, K. Nishinari, Simulation for pedestrian dynamics by real-coded cellular automata (rca), Physica A: Statistical Mechanics and its Applications 379 (2) (2007) 654–660. doi:10.1016/j.physa.2007.02.040.
URL http://dx.doi.org/10.1016/j.physa.2007.02.040

[34] C. M. Henein, T. White, Macroscopic effects of microscopic forces between agents in crowd models, Physica A: Statistical Mechanics and its

Applications 373 (2007) 694–712. doi:10.1016/j.physa.2006.06.023.
URL http://dx.doi.org/10.1016/j.physa.2006.06.023

[35] W. Weng, T. Chen, H. Yuan, W. Fan, Cellular automaton simulation of pedestrian counter flow with different walk velocities, Physical Review E 74 (3) (2006) 036102. doi:10.1103/PhysRevE.74.036102.
URL http://dx.doi.org/10.1103/PhysRevE.74.036102

[36] M. J. Seitz, G. Köster, Natural discretization of pedestrian movement in continuous space, Physical Review E 86 (4) (2012) 046108. doi:10.1103/PhysRevE.86.046108.
URL http://dx.doi.org/10.1103/PhysRevE.86.046108

[37] U. Weidmann, Transporttechnik der Fussgänger, no. 90 in 2, Institut für Verkehrsplannung, ETH Zürich, 1993.

[38] B. D. Oberhagemann, Static and Dynamic Crowd Densities at Major Public Events, Tech. Rep. March, Vereinigung zur Förderung des Deutschen Brandschutzes (2012).

[39] R. Verberg, A. Ladd, Lattice-boltzmann model with sub-grid-scale boundary conditions, Physical Review Letters 84 (10) (2000) 2148. doi:10.1103/PhysRevLett.84.2148.
URL http://dx.doi.org/10.1103/PhysRevLett.84.2148

[40] S. Hou, J. Sterling, S. Chen, G. Doolen, A lattice boltzmann subgrid model for high reynolds number flows, arXiv:comp-gasarXiv:9401004.
URL http://arxiv.org/pdf/cond-mat/9401004

[41] S. Chen, G. D. Doolen, Lattice boltzmann method for fluid flows, Annual review of fluid mechanics 30 (1) (1998) 329–364. doi:10.1146/annurev.fluid.30.1.329.
URL http://dx.doi.org/10.1146/annurev.fluid.30.1.329

[42] S. Nowak, A. Schadschneider, Quantitative analysis of pedestrian counterflow in a cellular automaton model, Physical Review E 85 (6) (2012) 066128. doi:10.1103/PhysRevE.85.066128.
URL http://dx.doi.org/10.1103/PhysRevE.85.066128

[43] L. Jian, Y. Lizhong, Z. Daoliang, Simulation of bi-direction pedestrian movement in corridor, Physica A: Statistical Mechanics and its Applications 354 (2005) 619–628. doi:10.1016/j.physa.2005.03.007.
URL http://dx.doi.org/10.1016/j.physa.2005.03.007

[44] Y. Yu, W. Song, Cellular automaton simulation of pedestrian counter flow considering the surrounding environment, Physical Review E 75 (4) (2007) 046112. doi:10.1103/PhysRevE.75.046112.
URL http://dx.doi.org/10.1103/PhysRevE.75.046112

[45] M. Muramatsu, T. Irie, T. Nagatani, Jamming transition in pedestrian counter flow, Physica A: Statistical Mechanics and its Applications 267 (3) (1999) 487–498. doi:10.1016/S0378-4371(99)00018-7.
URL http://dx.doi.org/10.1016/S0378-4371(99)00018-7

[46] F. Weifeng, Y. Lizhong, F. Weicheng, Simulation of bi-direction pedestrian movement using a cellular automata model, Physica A: Statistical Mechanics and its Applications 321 (3) (2003) 633–640. doi:10.1016/S0378-4371(02)01732-6.
URL http://dx.doi.org/10.1016/S0378-4371(02)01732-6

[47] K. Nishinari, A. Kirchner, A. Namazi, A. Schadschneider, Extended floor field ca model for evacuation dynamics, arXiv:cond-matarXiv:0306262v1.
URL http://arxiv.org/pdf/cond-mat/0306262

[48] C. Rogsch, A. Schadschneider, A. Seyfried, W. Klingsch, How to select the "right one"-update schemes for pedestrian movement in simulation and reality, in: Proceedings of the Traffic and Granular Flow, Vol. 9, 2009, p. 0.

[49] U. Wilensky, Netlogo (1999).

[50] C. Feliciani, K. Nishinari, Phenomenological description of deadlock formation in pedestrian bidirectional flow based on empirical observation, Journal of Statistical Mechanics: Theory and Experiment 2015 (10) (2015) P10003. doi:10.1088/1742-5468/2015/10/P10003.
URL http://dx.doi.org/10.1088/1742-5468/2015/10/P10003

[51] K. K. Finnis, D. Walton, Field observations to determine the influence of population size, location and individual factors on

pedestrian walking speeds, Ergonomics 51 (6) (2008) 827–842. doi:10.1080/00140130701812147.
URL http://dx.doi.org/10.1080/00140130701812147

[52] A. Seyfried, B. Steffen, W. Klingsch, M. Boltes, The fundamental diagram of pedestrian movement revisited, Journal of Statistical Mechanics: Theory and Experiment 2005 (10) (2005) P10002. doi:10.1088/1742-5468/2005/10/P10002.
URL http://dx.doi.org/10.1088/1742-5468/2005/10/P10002

[53] W. Alhajyaseen, H. Nakamura, Effects of bi-directional flow and different pedestrian age-groups on capacity of signalized crosswalks, in: Proceedings of Infrastructure Planning, Vol. 39, 2009, pp. 1–4.
URL http://library.jsce.or.jp/jsce/open/00039/200906_no39/pdf/79.pdf

[54] W. K. Alhajyaseen, H. Nakamura, Quality of pedestrian flow and crosswalk width at signalized intersections, {IATSS} Research 34 (1) (2010) 35–41. doi:10.1016/j.iatssr.2010.06.002.
URL http://dx.doi.org/10.1016/j.iatssr.2010.06.002

[55] D. Helbing, P. Mukerji, Crowd disasters as systemic failures: analysis of the love parade disaster, EPJ Data Science 1 (1) (2012) 1–40. doi:10.1140/epjds7.
URL http://dx.doi.org/10.1140/epjds7